Structure of cellulose and microcrystalline cellulose from various wood species, cotton and flax studied by X-ray scattering

Kirsi Leppänen · Seppo Andersson ·
Mika Torkkeli · Matti Knaapila ·
Nina Kotelnikova · Ritva Serimaa

Abstract The structure of microcrystalline cellulose (MCC) made by mild acid hydrolysis from cotton linter, flax fibres and sulphite or kraft cooked wood pulp was studied and compared with the structure of the starting materials. Crystallinities and the length and the width of the cellulose crystallites were determined by wide-angle X-ray scattering and the packing and the cross-sectional shape of the microfibrils were determined by small-angle X-ray scattering. The morphological differences were studied by scanning electron microscopy. A model for the changes in microfibrillar structure between native materials, pulp and MCC samples was proposed. The results indicated that from softwood or hardwood pulp, flax cellulose and cotton linter MCC with very similar nanostructures were obtained with small changes in reaction conditions. The crystallinity of MCC samples was 54–65%. The width and the length of the cellulose crystallites increased when MCC was made. For example, between cotton and cotton MCC the width increased from 7.1 nm to 8.8 nm and the length increased from 17.7 nm to 30.4 nm. However, the longest crystallites were found in native spruce wood (35–36 nm).

Keywords Microcrystalline · Cellulose · WAXS · SAXS

K. Leppänen · S. Andersson · M. Torkkeli ·
R. Serimaa (✉)
Division of Materials Physics, Department of Physics, University of Helsinki, P.O.B. 64, 00014 Helsinki, Finland
e-mail: serimaa@cc.helsinki.fi

M. Knaapila
MAX-lab, Lund University, P.O.B. 118, 22100 Lund, Sweden

Present Address:
M. Knaapila
Department of Physics, Institute for Energy Technology, P.O.B. 40, 2027 Kjeller, Norway

N. Kotelnikova
Institute of Macromolecular Compounds, Russian Academy of Sciences, Bolshoy pr. 31, St., 199004 Petersburg, Russia

Introduction

Demand for renewable resources has increased interest in cellulose and growing number of studies on applications of cellulose have been made. Natural fibres are used as microfibrillar fillers and composites in many applications including furnitures, irrigation systems, sports and leisure items (Samir et al. 2005). Microcrystalline cellulose (MCC) from various origins has been widely used in medical, food and cosmetic industrial applications. It has been utilized for example as a binder and filler in medical tablets, supporter for various biologically active substances, stabilizer in various suspensions, controller of flow and fat replacer in food (Fleming et al. 2001;

El-Sakhawy and Hassan 2007; Kotelnikova and Panarin 2005). Nanocrystalline cellulose whiskers have lately gained much attention because of their extraordinary properties which can be used in liquid crystalline suspensions and reflective pigments (Revol et al. 1992, 1994; Roman and Gray 2005; Terech et al. 1999; Elazzouzi-Hafraoui et al. 2008; de Souza Lima and Borsali 2004).

On the molecular level cellulose is a polymer which consists of $\beta(1,4)$-linked glucose residues (Sjöström 1993). The supramolecular structure of cellulose has been under investigations during the last 70 years. It is well known that crystalline cellulose (I) exists in nature in two main forms (triclinic I_α and monoclinic I_β) (Atalla and Vander- Hart 1984; Sugiyama et al. 1991; Nishiyama et al. 2002, 2003b). Some interesting details of the structure of cellulose are still unknown—for example, it is unknown what the connection between the cellulose crystallization and the biological cellulose synthesis complex is (Emons et al. 2007).

The wood cell wall consists of cellulose, hemicellulose and lignin (Sjöström 1993). Cellulose is the main component of the cell wall and its function is closely related to its hierarchical structure. In the cell wall the parallel cellulose chains form cellulose microfibrils which are bound to hemicellulose and lignin matrix. There are alternating amorphous and crystalline regions in the microfibrils (Nishiyama et al. 2003a; Gomez et al. 2008). The crystalline regions are called cellulose crystallites and they are formed by the cellulose chains due to Van der Waals interactions and hydrogen bonding. The diameter of these crystallites is of the same order as the diameter of the cellulose microfibrils (Donaldson 2007; Andersson 2007). The structure of the wood cell wall determines the strength of the fibres and this has impact on the applications and products made of wood. Changes in cellulose microfibrils and their aggregates occurring during pulping or the hydrolysis process have impact on the fibre properties and are important from the point of view of applications.

The aim of this work was to gain comparative information on the structures of the pristine plant and wood, pulp and MCC samples. In this work MCC was made from conventional plant and wood sources: cotton linter, flax fibres and sulphite and kraft cooked pulps from Scotch pine (*Pinus sylvestris*), Norway spruce (*Picea abies*), Silver birch (*Betula pendula*),

poplar (*Populus simonii*) and aspen (*Populus tremula*) wood. The effect of hydrolysis on the structure and properties of low molecular weight microcrystalline cellulose was estimated. The nanometer scale structure of cellulose microfibrils was characterized using wide- and small-angle X-ray scattering methods (WAXS, SAXS). Scanning electron microscopy (SEM) was used to study the morphological differences in the materials. On the basis of the results, a model for the changes in microfibrillar structure between native wood or plant material, pulp and MCC was proposed.

Experimental

Materials

Norway spruce samples were cut tangentially from stems grown in Asa in Southern Sweden (Andersson 2007; Lundgren 2004). The samples were cut into 1 mm thick slices with about 1 cm × 1 cm area. The samples were taken from the 14th year ring and they represented mature wood. Sample called ASA12 was from an irrigated and fertilized stem and ASA13 was its control sample from a stem, which was not irrigated or fertilized.

Pine and spruce wood celluloses were purchased from the Academy of Forestry (St. Petersburg, Russia). Pine and spruce wood celluloses were manufactured in industrial plants using ordinary pulping processes, which were performed with a mixture of sodium hydroxide and sodium sulfide (NaOH and Na_2S) that break the bonds of lignin to cellulose (kraft process) or with various salts of sulphurous acid (mostly sodium bisulphate $NaHSO_3$ or sodium sulphate Na_2SO_3) to extract the lignin from wood samples (sulphite pulping). Characteristics including cellulose and lignin content and kappa numbers of the pulp samples are given in the Table 1. MCC from pine and spruce pulp was prepared by hydrolysis in 1 M solution of HCl at 105 °C for 2 h (Kotelnikova et al. 1976).

Birch wood cellulose was prepared by the same sulphite cooking process as explained earlier with pine and spruce celluloses. Birch cellulose was made from birch chips and was formed into sheets. Cellulose was subjected to alkaline treatment with a 10% solution of NaOH at 100 °C to remove hemicelluloses. After this, the pulp was washed with

Table 1 Characteristics of cellulose and MCC samples: cellulose and lignin content, kappa number (for pulp samples), degree of polymerization (DP), average fibre length and specific surface

Sample	Cellulose content (mass%)	Lignin content (mass%)	Kappa number	DP	Average fibre length (μm)	Specific surface (m^2/g)
Birch sulphite pulp	95.8	1.4	9.8	1600	500–1500	230
MCC from						
Birch sulphite pulp	97.3	0.5		175	20–100	250
Coniferous sulphite pulp	96.2	1.3	8.7	1310	400–1700	270
MCC from						
Coniferous sulphite pulp	98.8	0.4		275	80–185	280
Coniferous kraft pulp	97.8	1.1	7.5	1135	500–2100	280
MCC from						
Coniferous kraft pulp	98.6	0.5		150	60-165	290
Poplar kraft pulp	96.4	1.2	8.2	1300	750–850	210
MCC from						
Poplar kraft pulp	97.6	0.8		250	90-95	220
Aspen kraft pulp	96.8	1.0	6.7	1250	800–1100	220
MCC from						
Aspen kraft pulp	97.5	0.6		230	50–60	240
Cotton linter (CL)	98.5	0.7		2200	2150	220
MCC from CL	99.8	0		165	20–125	230
Flax fibres (FF)	78.5	7.8		5600	1500–14500	600
Cellulose from FF	97.9	1.2		470	550–600	490
MCC from FF cellulose	99.6	0		170	30–150	510
MCC "Avicel"	99.9	0		150	20–250	–

distilled water overnight and dried in vacuum at 40 °C. MCC from birch cellulose was prepared by hydrolysis in 1 M of HCl at 105 °C for 1.5 h (Petropavlovsky et al. 1980).

Cellulose samples from aspen and poplar wood (origin in China) were prepared by kraft cooking and bleached after pulping. Cooking was performed in a laboratory forced circulation digester with a cooking vessel volume of 5 dm^3 and a circulation flow rate of 10 dm^3/s. Air-dried wood chips were mixed with cooking liquor. Cooking liquor was prepared from technical grade Na_2S and NaOH to reach the alkalinity of 16% and sulphidity of 28%. The liquor-to-wood ratio (w/w) during pulping was 6:1. The initial temperature of 30 °C was raised to 165 °C at a heating ratio of 1.0 °C/min and maintained at this temperature for 180 min. The pulps were washed with hot water and the rest of liquor was released by washing through a 250-mesh wire. A bleaching

sequence was made as follows. First pulp (concentration 3.5%) was treated with an aqueous chlorine solution (chlorine consumption 1.5%) at 30 °C for 1 h. Then it was treated with 1% solution of NaOH at pulp concentration of 8.0% at 70 °C for 1 h. Then pulp (concentration 3.5%) was additionally bleached with NaClO (chlorine consumption 0.5%) at 30 °C for 40 min. Finally pulp (concentration 3.5%) was treated with 0.2% solution of HCl for 30 min. After thorough rinsing with tap water pulp was ready to further study. MCC from aspen and poplar bleached celluloses were obtained by hydrolysis in 1 M solution of HCl at 105 °C for 2.5–3.0 h (Kotelnikova et al. 1991).

Cotton linter was purchased from an industrial plant (Tashkent, Republic of Uzbekistan). It was used without any additional purification. MCC was prepared by mild acid hydrolysis in 2.5 M solution of HCl at 105 °C for 1 h (Petropavlovsky and

Kotelnikova [1985]). Avicel powder cellulose produced by FMC Corporation (New Jersey, USA) was used for comparison. Flax fibres were purchased from the flax treating plant (Nevel, Russia). Cellulose from flax fibres was prepared after purification and delignification and was a fibre sample (Kotelnikova et al. [2000]). MCC from flax cellulose was obtained the same way as described above for birch cellulose.

MCC samples were prepared from the initial raw materials to so called level-off degree of polymerization (Battista [1975]). After hydrolysis MCC samples had powder-like morphology and consisted of rod-shaped particles whose sizes were from 1.5 to 150 μm depending on the initial raw material. Some characteristics of the raw materials and MCC samples—cellulose and lignin content, degree of polymerization (DP), average fibre length and an important adsorption property, specific surface—are listed in Table [1]. DP values were determined by viscosimetry of cellulose solutions in cadoxen. Values of the specific surface area were obtained with a method of aqueous vapor sorption (Buckton et al. [1999]; Zografi et al. [1984]). Specific surface was determined with Brunauer–Emmet–Teller (BET) equation which describes the isotherm of adsorption in the range p/p_s from 0.05 to 0.3. It can be seen from the data on cellulose and lignin contents in cellulose samples in Table [1] that hemicelluloses were mostly absent.

WAXS experiments

WAXS measurements were done using Huber 420/511 four-circle goniometer. A ground and bent germanium monochromator (the reflection 111) was used to select $CuK\alpha_1$ radiation ($\lambda = 0.1541$ nm). The scattered photons were detected by a NaI(Tl) scintillation counter. The diffractometer was used in the symmetrical transmission mode and the intensity was measured as a function of the scattering angle 2θ by $\theta - 2\theta$ scan. The instrumental broadening was determined from the FWHM of four reflections of a sample of hexamethylenetetramine ($C_6H_{12}N_4$). The reflections 110 ($2\theta \approx 17.8°$), 200 ($2\theta \approx 25.3°$), 211 ($2\theta \approx 31.1°$), and 220 ($2\theta \approx 36.1°$) of $C_6H_{12}N_4$ were used (Lofty et al. [1974]; Tanaka et al. [1981]).

For spruce wood samples ASA12 and ASA13 WAXS measurements were carried out using perpendicular transmission geometry and Rigaku

rotating anode X-ray tube. MAR345 image-plate was used as a detector. The beam was focused to the detector and monochromated with a Si(111) crystal and a totally reflecting mirror. The wavelength of the radiation was 0.1541 nm ($CuK\alpha_1$).

SAXS experiments

SAXS measurements were carried out at the beamline I711 at MAX-lab in Lund, Sweden (Knaapila et al. [2009]). The wavelength of the radiation was 0.1083 nm, the beam size was 0.12 mm × 0.12 mm and it was focused on the detector. The detector was two-dimensional Mar165 CCD and the distance from the sample to the detector was 1.5 m. The measurement time was 180–360 s. The applied q-range ($q = 4\pi \sin\theta/\lambda$) was 0.1–4.0 nm^{-1}.

The samples which were measured by SAXS included Norway spruce wood samples ASA12 and ASA13, sulphite cooked birch pulp, sulphite and kraft cooked pulp from spruce and pine, cotton linter, flax fibres and cellulose from flax fibres. The samples needed to be wet during the measurements to reduce the scattering from air filled pores, so the samples were sealed with water in Hilgenberg glass capillaries with 0.01 mm wall thickness and 2 mm path length many days before the measurements.

SEM

Morphological features of cellulose and MCC fibres were characterized with scanning electron microscopy (SEM). Micrographs were taken with a LEITZ/AMR 1200B and a Jeol JCM-35 CF scanning electron microscopes at 15 and 20 kV voltage. Dry samples were mounted on aluminum stubs covered by carbon ribbon, then sputtered under argon atmosphere using a gold-palladium target.

Data analysis

WAXS analysis

The WAXS intensities were corrected for absorption and air scattering. The dimensions of the crystallites were determined along the cellulose chain direction by using the meridional reflection 004 and perpendicular to the chain direction by using equatorial reflections 110, 1$\bar{1}$0 and 200. In the analysis of the

reflections $110, 1\bar{1}0$ and 200 the amorphous background was fitted to the experimental intensity pattern and subtracted. The amorphous background was measured from a sulphate lignin sample (Andersson et al. 2003). In the analysis of the reflection 004 the background was assumed constant. Gaussian peaks were fitted into the diffraction pattern and the average crystallite width B_{hkl} was determined from the FWHM (full width at half maximum) of the diffraction peaks by using the Scherrer equation:

$$B_{hkl} = \frac{0.9\lambda}{\sqrt{(\Delta 2\theta)^2 - (\Delta 2\theta_{inst})^2} \cos\theta}, \quad (1)$$

where λ is the wavelength of the radiation, $\Delta 2\theta$ is the FWHM of the reflection, 2θ is the position of the reflection in the scattering angle axis and $\Delta 2\theta_{inst}$ is the instrumental broadening. The fitted amorphous background and Gaussian peaks for cotton linter can be seen in the Fig. 1.

The crystallinity index was determined by a curve fitting procedure where the calculated diffraction pattern of cellulose and a measured diffraction pattern of amorphous material were fitted into the experimental diffraction pattern (Andersson et al. 2003).

SAXS analysis

SAXS gives information on the packing of the microfibrils and the cross-sectional shape and size
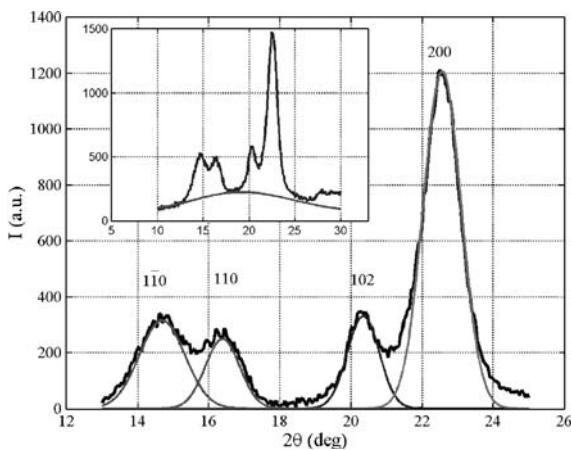

Fig. 1 WAXS intensity of cotton linter and fitted Gaussian functions to the reflections $110, 1\bar{1}0, 102$ and 200. The fitted amorphous background can be seen in the *insert*

of the microfibrils. In a simple way the SAXS intensity $I(q)$ can be presented as:

$$I(q) = C\frac{1}{q}|F(q)|^2 Z(q) + BG, \quad (2)$$

where $F(q)$ is the form factor, which depends on the shape of the microfibril, and $Z(q)$ is the interference factor, which depends on the packing of the microfibrils (Feigin and Svergun 1987; Wilke and Bratrich 1991). C is a scaling factor and BG is a background constant. They both were kept as fitting parameters (Andersson et al. 2005). Microfibrils were modelled by crystalline, infinite long cylinders with rectangular, circular or elliptical cross-section with or without Gaussian or log-normal size distribution. The fitted q-range was about 0.95–3.5 nm^{-1}. It was chosen so, because it was assumed that the region $q < 0.9$ nm^{-1} corresponds to the region where scattering mainly arises from the pores, the scattering in the region $q = 0.8$–2.3 nm^{-1} is from the crystallites, and the scattering in the region $q > 2.3$ nm^{-1} is from amorphous structures (Andersson et al. 2005; Jakob et al. 1995, 1996; Andersson et al. 2000). For the spruce wood samples a two-dimensional paracrystal model was used as an interference function $Z(q)$, and the mean distances between the microfibrils and the mean diameters of the cross-sections of the microfibrils were gained as fitting parameters. For the other samples the interference term $Z(q)$ could be omitted, because the intensity curves showed no features connected to packing. Only the shapes and the mean diameters of the cross-sections of the microfibrils could be determined for these samples.

The square of the form factor for a cylinder with circular cross-section is:

$$|F(q)|^2 \propto \frac{J_1(qr)^2}{(qr)^2}, \quad (3)$$

where J_1 is the Bessel function of the first kind and r is the radius of the cylinder (Feigin and Svergun 1987).

For a parallelepiped the following formula is used:

$$|F(q)|^2 \propto \int_0^{\pi/2} \left(\frac{\sin(q\frac{a}{2}\sin(\phi))}{q\frac{a}{2}\sin(\phi)}\right)^2 \left(\frac{\sin(q\frac{b}{2}\cos(\phi))}{q\frac{b}{2}\cos(\phi)}\right)^2 d\phi, \quad (4)$$

where a and b are the edges of the rectangular cross section (Pedersen 1997; Elazzouzi-Hafraoui et al. 2008). The model of the microfibrils with rectangular

cross section can be seen in the Fig. 2 where the parameters a and b are the edges of the rectangle and d is the mean distance between the microfibrils.

The function modelling a two-dimensional para-crystal, which was used as an interference function, is:

$$Z(q) \propto \int\limits_0^{\pi/2} \frac{1 - F_1^2}{1 - 2F_1 \cos(-qd_1 \cos\phi) + F_1^2} \frac{1 - F_2^2}{1 - 2F_2 \cos(qd_2 \sin\phi) + F_2^2} d\phi, \tag{6}$$

For cylinders with elliptical cross-sections the square of the form factor was computed as:

$$|F(q)|^2 \propto \int\limits_0^{\pi/2} \frac{J_1(qr\sqrt{\sin^2(\phi) + b^2\cos^2(\phi)})^2}{(qr\sqrt{\sin^2(\phi) + b^2\cos^2(\phi)})^2} d\phi, \tag{5}$$

where r and rb are the semiaxes of the ellipse (Feigin and Svergun 1987). The model of the microfibrils with elliptical cross sections can be seen in the Fig. 3, where the parameters a and b are the semiaxes of the ellipse and d is the mean distance between the microfibrils.

$$F_1(q) = \exp\left(-\frac{1}{2}g_1^2 d_1^2 q^2\right), \tag{7}$$

$$F_2(q) = \exp\left(-\frac{1}{2}g_2^2 d_2^2 q^2\right), \tag{8}$$

where d_1 and d_2 are the mean distances between the microfibrils in two perpendicular directions, and g_1 and g_2 are the relative values of the fluctuations in corresponding directions. The g parameter characterizes the order of the structure, and the closer to one its value is, more weakly ordered the system is in that direction. Small values of g indicate a well
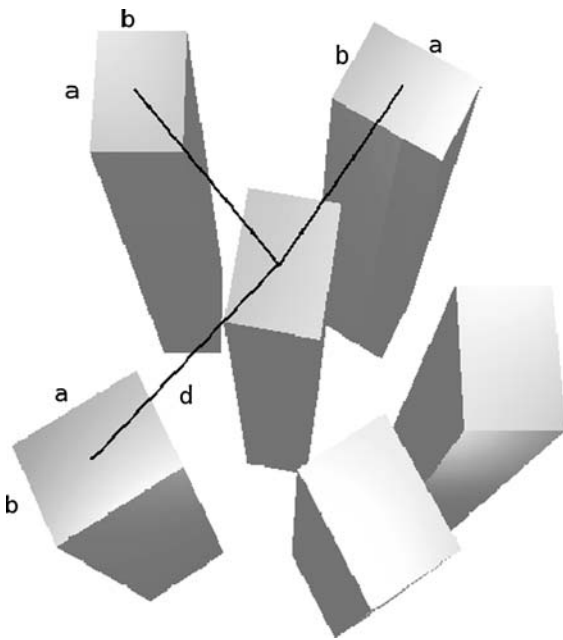

Fig. 2 Microfibrils with rectangular cross section. d is the mean distance between the microfibrils and a and b are the edge lengths of the cross section
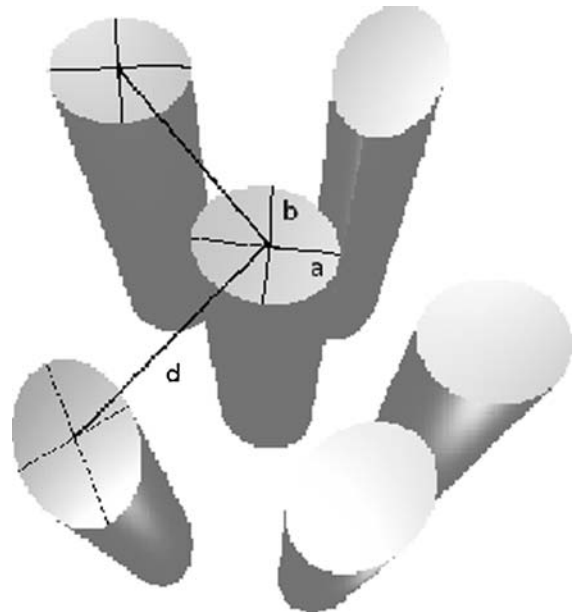

Fig. 3 Microfibrils with elliptical cross section. d is the mean distance between the microfibrils and a and b are the semiaxes of the cross section

ordered system and $g > 0.3$ indicates already very disordered system (Wilke and Bratrich 1991). The Eqs. 6–8 are valid only when the following assumptions can be made: the size of the paracrystal is infinitely large, and the two directions in the cross-sectional area are independent on each other (Matsuoka et al. 1987).

Results

WAXS results on crystallite size and crystallinity

The average length of the cellulose crystallites was determined from the reflection 004 for all samples. For samples with sufficiently well resolved equivatorial diffraction peaks, the width of the crystallites was determined from the reflections 200, $1\bar{1}0$, and 110. For samples with broad diffraction peaks, like spruce wood, only the reflection 200 could be used. All the WAXS results are given in the Table 2.

The width of the crystallites in the spruce wood samples was 3.0 ± 0.1 nm, and the length of the crystallites was 35 ± 2 and 36 ± 2 nm (Andersson 2007). The width of the crystallites in cotton linter was 7.1 ± 0.2 nm and in flax fibres 3.9 ± 0.1 nm. So, this parameter is higher in non-wood plant samples than in wood samples.

The widths of the crystallites in kraft and sulphite wood pulps (4.3 ± 0.1, 4.4 ± 0.1 and 5.1 ± 0.1 nm) were larger than the widths in native spruce wood. The lengths of the crystallites in wood pulp samples were smaller than the lengths in the wood samples: 23.3 ± 2 nm in birch sulphite pulp, 26.3 ± 2 nm in coniferous sulphite pulp and 22.8 ± 2 nm in coniferous kraft pulp. Crystallites in cellulose from flax fibres had larger width than in pristine flax. Also the length of the crystallites increased compared to the initial flax fibres.

The width and length of the crystallites in the MCC samples made from kraft and sulphite cooked fibres and cotton were larger than the corresponding dimensions in the starting materials. The length of the crystallites of cotton MCC increased about 72% compared to pristine cotton linter, whereas increase for other MCC samples was in the range from 2 to 20%. Exceptions to this were the length of the MCC crystallites made from birch sulphite pulp (a little lower) and from flax cellulose (the crystallite width

Table 2 The dimensions B_{200}, $B_{1\bar{1}0}$, B_{110} and B_{004} of cellulose crystallites (nm) that were determined parallel and perpendicular to the cellulose chain axes by using equatorial reflections 200, $1\bar{1}0$ and 110 and the meridional reflection 004

Sample	Crystallinity (%)	B_{200}	$B_{1\bar{1}0}$	B_{110}	B_{004}
ASA12 spruce wood	–	3.0	–	–	35.0
ASA13 spruce wood	–	3.0	–	–	36.0
Birch sulphite pulp	52	4.3	4.7	4.3	23.3
MCC from Birch sulphite pulp	54	4.6	5.0	4.3	21.9
Coniferous sulphite pulp	58	4.4	4.6	4.4	26.3
MCC from Coniferous sulphite pulp	59	5.3	5.3	4.8	26.8
Coniferous kraft pulp	50	5.1	3.8	3.1	22.8
MCC from Coniferous kraft pulp	63	5.7	5.4	4.6	27.3
MCC from Poplar kraft pulp	60	4.8	4.5	5.4	19.8
Aspen kraft pulp	63	5.1	4.6	5.7	–
Cotton linter (CL)	–	7.1	4.7	6.3	17.7
MCC from CL	65	8.8	5.2	7.4	30.4
Flax fibre (FF)	–	3.9	3.2	4.2	17.8
Cellulose from FF	–	4.7	3.1	5.4	21.1
MCC from FF cellulose	60	4.7	3.8	5.6	23.7
MCC "Avicel"	59	5.0	–	–	24.9

B_{004} values for the spruce wood samples ASA12 and ASA13 are from Andersson (2007)

was equal). The difference between the sulphite or kraft cooked samples and MCC samples made from these starting materials was not large, except in the case of coniferous kraft pulp. The WAXS intensities for coniferous kraft pulp, MCC made from it, birch sulphite pulp and MCC made from it can be seen in the Fig. 4.

The crystallinity of the MCC samples was 54–65%. For the MCC samples made from sulphite pulp samples the crystallinity did not change much compared to the starting materials, but for coniferous kraft cellulose the difference between crystallinity of the pulp sample and the MCC sample was more than 10%-units. The highest crystallinity (65%) was determined for the MCC sample prepared from cotton.

Fig. 4 *Curves top down*: WAXS intensities of coniferous kraft cellulose, MCC made from it, birch sulphite cellulose and MCC made from it
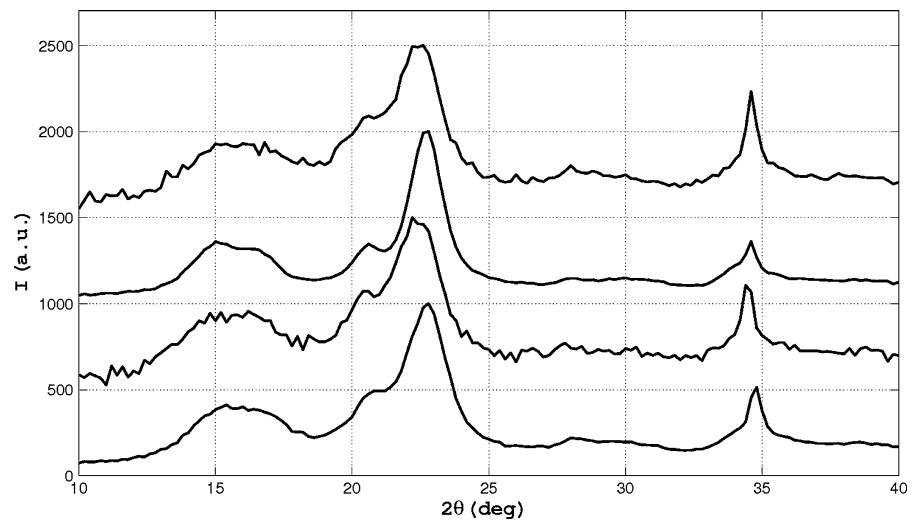
SAXS results on the packing, cross sectional size and shape of the microfibrils

The SAXS intensities of the spruce wood samples showed features of the packing of the microfibrils, so the SAXS intensities were analyzed using a model of two-dimensional paracrystal (Eq. 6) as an interference term. The microfibrils were modelled as infinite long cylinders with circular cross-sections. The fitting results for the samples ASA13 and ASA12 are given in the Table 3: g_1 and g_2 are the order parameters, and the mean distances between the microfibrils in two directions are given in the corresponding order. The values of the g-parameters were high indicating that the packing of the microfibrils was not very well ordered. The value of g parameter was higher in the direction which corresponds to the larger mean distance. The experimental and fitted SAXS intensities can be seen in the Fig. 5.

The SAXS intensities of all the other samples could be interpreted in terms of scattering from individual microfibrils. The SAXS intensity of birch sulphite pulp was analyzed by a model where the microfibrils were cylinders with elliptical cross-sections with Gaussian size distribution. Also other models were tried using rectangular and circular cross sections. However, the results indicated that the cross-section is very close to circular (Table 3).

Cylinders with circular cross-sections gave the best fitting results also for the both pulp samples from coniferous wood. The diameters are given in the

Table 3. These values are remarkably low compared to the WAXS results (Table 2). The experimental and fitted SAXS intensities for birch sulphite, coniferous sulphite and kraft cellulose can be seen in the Fig. 6.

The SAXS results of cotton linter were analyzed using the model of cylinders with rectangular and elliptical cross-section for the microfibrils. The difference between the analytical curves calculated using exactly same values for the fitting parameters for these two models was quite small. So both of the models gave the same results and it can be said that it is impossible to distinguish between these two models. The best fitting result was gained by assuming a log-normal size distribution for the edges of the rectangle or the semiaxes of the ellipse. Also Gaussian size distribution was tested, but the fitting results were not that good. The result for the edges/semiaxes are given in the Table 3. The standard deviation is significantly higher in the other direction, which means, that in this direction the crystalline region is not as well ordered as in the other.

The SAXS intensity of flax fibres was fitted best by the model of cylinders with elliptical cross-sections with Gaussian size distribution. The shape of the cross section of the microfibril was very elongated according to the results. The SAXS result of cellulose from flax fibres was analyzed using the same model. The cross section of the microfibril in the isolated cellulose sample is a little bit smaller and closer to circular shape than in pristine flax fibres.

Table 3 The results of the SAXS analysis

Sample	Shape of microfibril	Diameter of circle/axes of ellipse/edges of rectangle (nm)	g_1; g_2	Mean distance (nm)
ASA 13 spruce wood	Circular; 2d-paracryst.	2.6	0.5; 0.3	3.9; 3.5
ASA 12 spruce wood	Circular; 2d-paracryst.	2.5	0.5; 0.4	4.2; 3.5
Birch sulphite pulp	Elliptical	2.5 ± 0.3; 2.4 ± 0.3		
Coniferous sulphite pulp	Circular	2.5		
Coniferous kraft pulp	Circular	2.4		
Cotton linter	Rectangular	7.0 ± 0.8; 4.0 ± 1.8		
Flax fibres (FF)	Elliptical	3.8 ± 0.9; 2.1 ± 0.5		
Cellulose from FF	Elliptical	3.2 ± 0.5; 2.1 ± 0.3		

If the Gaussian or log-normal size distribution was included in the fitted model, the standard deviation is given with the size of the axes/edges. Mean distance could be given, if the interference term was used in the analysis
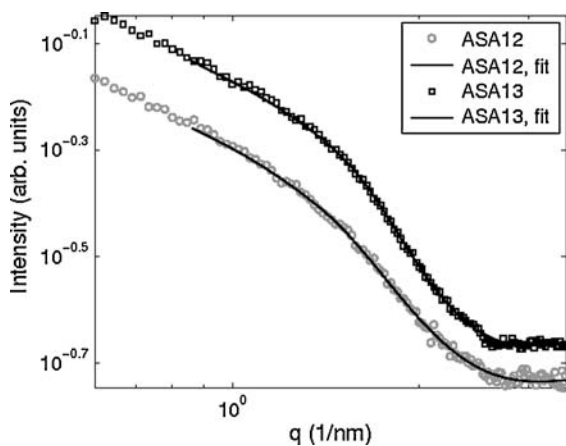

Fig. 5 Integrated SAXS intensities for Norway spruce wood samples ASA12 and ASA13 with the fitting results. Both axes are in logarithmic scale
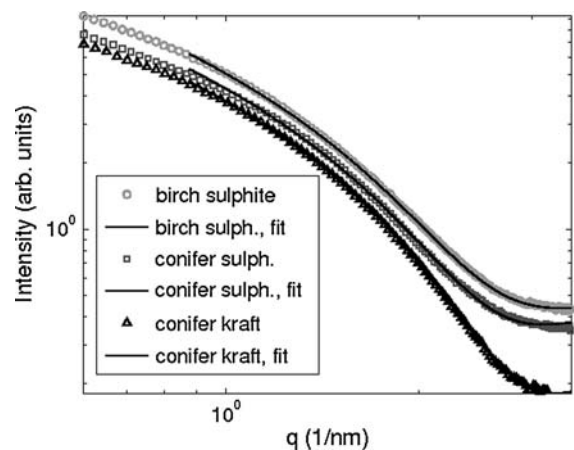

Fig. 6 Integrated SAXS intensities for coniferous sulphite, coniferous kraft and birch sulphite celluloses with the fitting results. Both axes are in logarithmic scale

SEM results on the morphological features of the fibres

Figure 7 reveals the morphological changes between the original flax fibres, cellulose made from flax fibres and MCC made from flax cellulose. The original flax fibres had a clear parallel orientation. When pulp was made from these fibres, the fibres formed bundles like the one shown in subfigure A2. In the MCC sample the fibres were less rod-like and less parallel with each other and the surface of the fibres was degraded due to the acid treatment. This can be seen also in the subfigures B1–B3, where MCC from cotton linter, birch sulphite pulp and poplar kraft pulp are presented.

Discussion

In this work nanometer scale structures of cellulose microfibrils of the native starting materials, pulp and MCC samples were characterized using X-ray scattering methods and differences were found in both sizes of cellulose crystallites and their packing. Differences also in the morphology of the original and modified samples in micrometer level were observed using SEM. These results are discussed in conjunction with the results of chemical studies (Table 1) and previous Fourier transform infra-red (FTIR) results for materials subjected to the same chemical treatments as the studied samples (Petropavlovsky et al. 1980; Kotelnikova et al. 1991;

Fig. 7 SEM graphs: (**A1**) original flax fibres; (**A2**) cellulose from flax fibres; (**A3**) MCC from cellulose from flax fibres; (**B1**) MCC from cotton linter; (**B2**) MCC from birch sulphite pulp; (**B3**) MCC from poplar kraft pulp. The length of the *scale bar* is 10 μm in all the figures
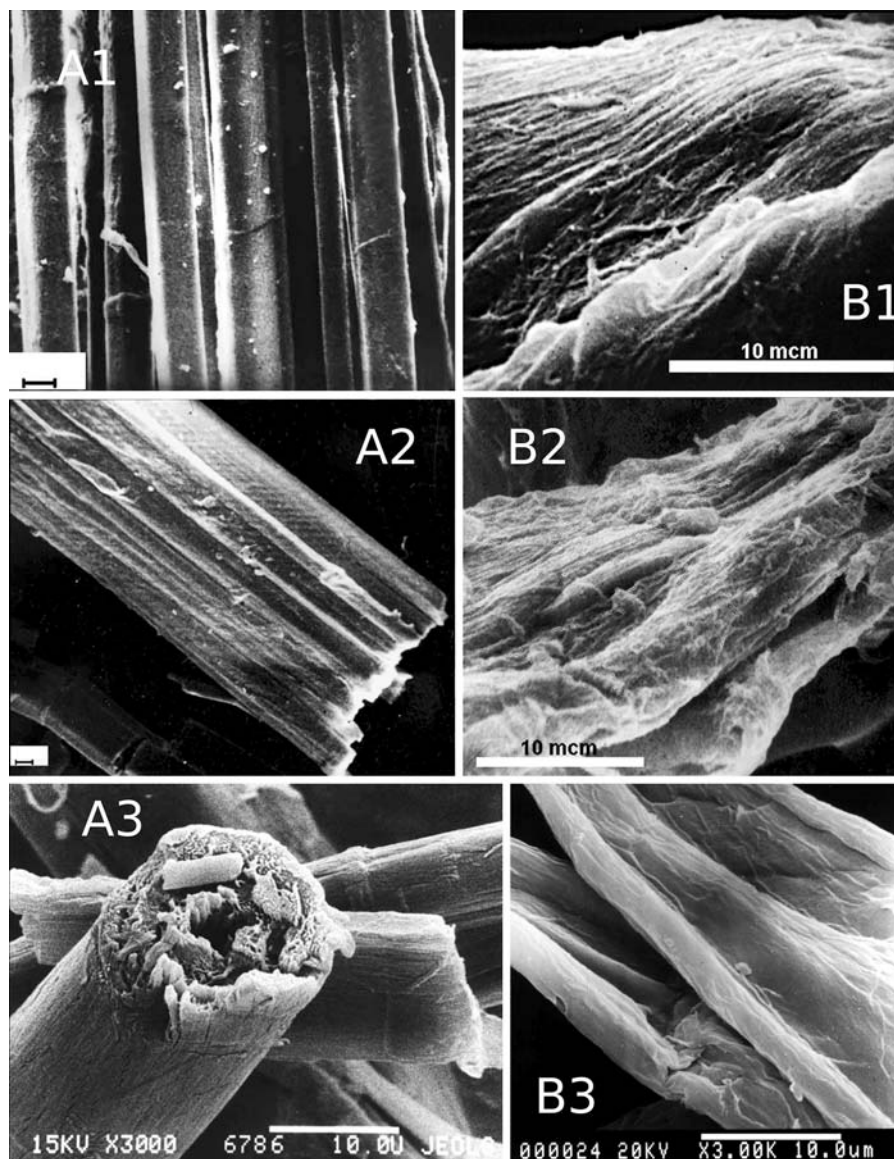
Petropavlovsky and Kotelnikova 1985; Kotelnikova et al. 2000).

FTIR spectroscopy monitors the chemical composition of samples and agrees with the removal of lignin during the chemical modifications. FTIR is also sensitive to changes in the hydrogen bonding network, which may happen e.g. during degradation or recrystallization of the microfibrils. The FTIR spectra of cellulose samples reveal the most intensive bands in the ranges 800–1800 cm^{-1}, 2850–2940 cm^{-1} and 3000–3600 cm^{-1}. The intensive bands in the first part of spectra have maxima located in the ranges 895–910 cm^{-1} (deformation vibrations of C1–H and asymmetric stretching vibrations of pyranose rings), 985–1200 cm^{-1} (stretching vibrations of CO groups, asymmetric stretching vibrations of pyranose rings and asymmetric stretching vibrations of bridge C1–O–C4 bonds), 1370 cm^{-1} (stretching vibrations of C–H), and 1430 cm^{-1} (symmetric stretching vibrations of C–H2 groups) (Krässig 1993). In the range 2800–2950 cm^{-1} there are two bands with maxima at 2850 and 2900 cm^{-1}, which are attributed to stretching symmetric and asymmetric vibrations of CH$_2$ groups. The range 3000–3600 cm^{-1} is formed by superposition of oscillations of OH-groups band, which are involved

in intra- and intermolecular H-bonds in cellulose chains. The range 3200–3300 cm^{-1} is assigned to stretching vibrations of intermolecular H-bonds such as O(6)H···O(3), and the range 3300–3600 cm^{-1} to stretching vibrations of intramolecular H-bonds such as O(3)H···O(6) and O(2)H···O(6) (Fengel 1993).

Wood samples

The width of the cellulose crystallites has been determined to be between 2.5 and 3.4 nm (Andersson et al. 2003, 2005; Jakob et al. 1995, 1996; Peura et al. 2007) for pine and spruce wood and 2.8 nm for Silver birch wood (Peura et al. 2009). Thus, the WAXS result for the spruce wood samples ASA12 and ASA13, 3.0 nm, corresponds well with the previous results for wood. It also corresponds well with the number of the cellulose chains originated in the biological cellulose synthesis complex (one rosette generates 36 chains, Doblin et al. 2002; Gomez et al. 2008).

Microfibrils consist of alternating crystalline and amorphous regions and for the spruce wood samples the length of the crystalline region was about 35 nm (Andersson 2007). The crystallites were in wood samples longer than in any other studied sample (Table 2).

The diameter of crystalline regions in microfibrils determined from SAXS data was slightly smaller than the width of the crystallites determined by WAXS. This difference of 0.4–0.5 nm is about the same as the distance of hydrogen bonded sheets of cellulose chains in a cellulose crystallite (Fig. 9). Thus, according to WAXS an average crystallite contains about eight parallel sheets of cellulose chains and according to SAXS there are seven of those sheets in the microfibril. SAXS detects the crystalline core of the microfibril. If the diameter of the core varies, SAXS gives an average diameter of the core. The width of the diffraction peaks in the WAXS pattern depends not only on the size of the crystallites and instrumental effects, but also on the perfection of the crystallites and possible strains in the crystallites. Around the crystalline part of the microfibril there is a layer of weakly ordered surface chains, part of which are bound to hemicellulose. Lattice distortions and amorphous regions follow from malfunctions of the cellulose synthesis complex like termination of chain formation. The smaller value of the diameter can be caused by these lattice imperfections and amorphous regions along the microfibril. In this point of view, it can be said that WAXS result is the lowest boundary for the size of the crystallite. But it is also known that WAXS is the most sensitive for the large well-ordered crystallites which give well defined diffraction peaks, so in this point of view WAXS result does not give the lowest boundary for the average size of the crystallites.

The obtained value of 3.5–4.2 nm for the mean distance between the microfibrils is reasonable compared to the diameters of the microfibrils. It is lower than the previous results for thermally modified pine samples analyzed by Andersson et al. (2005), but in the thermal modification the size of the crystallites increased and changes occurred also in the amorphous matrix, which can cause the difference between the results.

Here a two dimensional paracrystal model was used as the interference function. Wilke (1983) has presented general lattice factor of the ideal paracrystal and as a special case he calculated the case of a monoclinic macrolattice. This model has been used in studies of partially oriented polymers like polyethylene (Fronk and Wilke 1985; Wilke and Bratrich 1991). In this work a simplified version of the general lattice factor was found out to describe satisfactory the packing of microfibrils in the studied spruce wood samples. However, it should be noted that there exist also other possible models. For example, Busson and Doucet (1999) have calculated an analytical interference function for two-dimensional hexagonal paracrystals, which has been used in the analysis of keratin fibres (Briki et al. 1998). According to Mu et al. the size effect on the paracrystal diffraction has to be considered in the case of natural paracrystals (Mu 1998), but in our analysis the paracrystalline structure of the microfibrils was assumed to be infinite.

Wood pulp samples

The SAXS intensities of the pulp samples (Table 3) showed no features connected to the packing of the microfibrils and the interference function could be omitted from the SAXS analysis. The SAXS results indicated thus that the short range order between microfibrils is not as good as in native wood. Lignin is removed from the cell wall in the pulping process which makes the packing of cellulose microfibrils more irregular than in wood.

The width of cellulose crystallites determined from the reflection 200 in the WAXS pattern of the kraft or sulphite cooked samples was larger than that of wood samples: 4.3 and 4.4 nm for birch sulphite and coniferous sulphite cellulose, respectively, and 5.1 nm for coniferous kraft cellulose. This can be explained by the cooking process: when cellulose is isolated from wood tissue by kraft or sulphite cooking, hemicellulose and lignin are removed from the cell wall and this allows the surface chains of microfibrils to crystallize further. It is also possible that there exist separate cellulose chains, which can cling to the crystallites during the cooking process.

Also aggregation of the microfibrils in transverse direction during the isolation of cellulose by cooking process may occur. This has been proposed by Ioelovich (Ioelovich 1992), who made a WAXS study on native birch, pine and spruce wood samples and kraft or sulphite cooked pulp from the corresponding wood materials. His results for the average crystallite width of the native spruce and pine were 3.4 and 3.3 nm, respectively, and for the sulphite cooked spruce and pine 4.8 and 4.6 nm, respectively (Ioelovich 1992). Our results indicate that on average two crystallites have aggregated together during the cooking process.

For the kraft or sulphite cooked samples the width of the crystallites obtained by WAXS is larger than the microfibril diameter obtained by SAXS. This difference could be due to partial deterioration of the microfibril in the pulping process and points to the thinner and thicker parts in the microfibril in the kraft or sulphite cooked samples. According to Salmén (2004) the structure of the three dimensional web of the cellulose microfibrils and microfibril aggregates in pulp is lenticular so that the microfibrils have undulating behaviour. This could be a proper explanation for the difference between WAXS and SAXS results, because WAXS is more sensitive to the larger ordered areas like contact zones in the web of microfibrils and SAXS detects the sizes of the separate crystalline microfibrils. Also Kato et al. (1999) have used this kind of structural model, when they studied the wetting and drying of the cellulose fibres.

According to the WAXS results the crystalline regions of the microfibrils are longer in native wood than in the kraft or sulphite cooked samples. The decrease in length of the crystalline regions of microfibrils during the cooking process can be connected to the dramatic decrease of the DP (DP values in the Table 1 compared to the DP value of 10,000 in native wood, Sjöström 1993). The intensive chemical and physical treatments and high temperature during the pulping which is necessary for the separation of cellulose from lignin reduces the cellulose chain length. Probably also the decrease in the length of the crystallites happens due to that. Similar results have been obtained previously by Peura et al. (2006). These authors noticed that kraft cooking caused widening and shortening of the cellulose crystallites compared to the sizes of the crystallites in native wood samples.

According to previous studies, FTIR spectra of cellulose from birch and kraft pulp from aspen and poplar wood were similar (Petropavlovsky et al. 1980; Kotelnikova et al. 1991). The bands in the range 3000–3600 cm^{-1} were symmetric and maxima intensities were at 3380, 3400 and 3410 cm^{-1}, respectively. The maxima in the same range for coniferous sulphite and kraft pulp were 3370, 3400 and 3420 cm^{-1}. These bands were not as symmetric as for birch, aspen and poplar pulp samples. All those samples were well purified and free of lignin because no bands assigned to lignin were found in the spectra.

Cotton linter and flax

Cotton linter was the purest sample among the original samples: it had the highest content of cellulose (98.5 mass%) and it contained 0.7 mass% of lignin. Cotton linter and flax fibres had also the highest DP values (Table 1). DP of flax fibres was 5600 and that of cotton linter was 2200.

According to the WAXS results of cotton an average crystallite contains roughly two times the number of the cellulose chains originated in the biological cellulose synthesis complex (Fig. 8). The crystallite size of flax fibres was smaller than that of cotton linter but larger than in wood. The cellulose content of cotton and flax was also much higher than that of wood, thus chains produced by neighboring rosettes may more easily mix in cotton and flax than in wood.

SAXS intensities indicated irregular packing of microfibrils in cotton and flax (Table 3), since no interference term was needed in SAXS analysis. In both cotton and flax the cross-sectional shape of the microfibrils was elliptical. The values of the largest

diameters of the cross sections obtained by SAXS were close to the crystallite widths obtained by WAXS for both samples. According to the SAXS results of cotton the standard deviation is higher in one direction, which means that the crystalline region is not as well ordered in this direction. The figure of the cross section of the crystallite (Fig. 8) explains this. Elazzouzi-Hafraoui et al. (2008) have studied the crystal structure of MCC made from cotton linter, and they used in their analysis also log-normal size distribution. According to our SAXS results, for cellulose from flax fibres the diameter of the crystalline part of the microfibril was smaller than the crystallite width by WAXS indicating that the thickness of the crystalline core varies along the microfibril. Astley et al. (2001) have made a SAXS study on the structure of flax fibres and according to them the cross-section of the microfibrils was 1.0×5.0 nm^2.

The position of the maximum in the range 3000–3600 cm^{-1} in FTIR spectrum of cotton linter was at 3430 cm^{-1}, and for flax fibres at 3427 cm^{-1} (Kotelnikova et al. 2000). For cotton the band was symmetric but for flax it was asymmetric and shifted to higher frequencies. This means that major OH groups in flax were included into intramolecular bonds. The intensive band in the spectra of flax in the range 1620–1750 cm^{-1} reflected the stretching vibrations of carbonyl groups belonging to lignin, which was contained in pristine flax (Table 1). Some of those groups were conjugated with aromatic rings and in this case the position was lower than 1700 cm^{-1}.
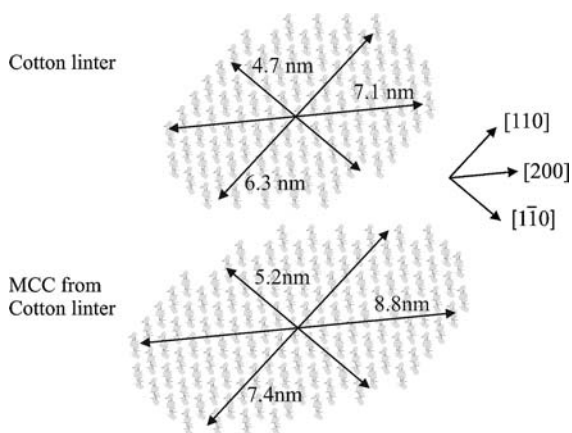

Fig. 8 A model for the cross section of the average crystalline region of the microfibril in cotton linter and that of the microfibril in cotton MCC

After delignification and bleaching of flax fibres, essential difference in the spectrum of cellulose from flax could be observed compared to the spectrum of pristine flax, i.e. the rearrangement of OH-groups band, which was splitted into two bands with maxima at 3285 and 3500 cm^{-1} (Kotelnikova et al. 2000). The intensity of the second band was lower than that of the first one. This indicated that cellulose from flax exhibited on average different system of OH-bonds compared to cotton and pulp samples. In flax cellulose the share of intramolecular hydrogen bonds had decreased and most of OH-groups were included into intermolecular H-bonds. This, probably, indicated that the intramolecular H-bonds in pristine flax fibres were not as stable as the intermolecular ones and they were mostly broken under delignification. The other difference of flax cellulose compared to flax fibres was that the bands in the range 1620–1750 cm^{-1} disappeared due to the removal of lignin during delignification.

MCC samples

All the MCC samples had high cellulose content: they contained 97.5–99.8 mass% of cellulose and not more than 0.6 mass% of lignin. The DP values of the MCC samples varied from 150 to 275. The crystallinity of MCC samples was 54–65%, so the samples had to include cellulose in amorphous form, which indicates that the cellulose microfibrils did not become single crystals. For both flax fibres and cotton linter the length of the crystallites increased and DP decreased considerably in the process of making MCC. However, the length of the crystallites remained shorter than the length of the polymer for all the studied samples. Between cotton and cotton MCC the increase in length was so significant, that the length of the crystallites in original cotton linter is explained rather by the lattice defects than by the large amorphous parts between the crystallites. The high cellulose content of cotton linter strengthens this interpretation.

Being very porous, flax MCC had the highest value of specific surface, 510 m^2/g, compared to the other MCC samples. This value is very high, which is seldom met for cellulose samples, and taking into account the powder morphology of MCC samples, this sample can be prospective for application as a sorbent. However, pristine flax fibres contained the

lowest mass fraction of cellulose (78.5 mass%) and the greatest mass fraction of lignin (7.8 mass%).

The crystallites were wider and longer in all the MCC samples than in the original samples, except in the case of birch sulphite cellulose. The changes in the widths of the crystallites were from 6.5 to 24%, so that the largest increase was observed in the case of cotton linter. Figure 8 illustrates the change in the cross section of the average crystalline region in a microfibril of cotton linter when MCC from it was prepared. In the Fig. 9 the same comparison is made between birch wood, birch sulphite pulp and MCC made from birch pulp.

The increase in the length of crystalline regions of the microfibrils was from 2 to 72%. One glucose ring is about 0.5 nm long so for MCC made from coniferous sulphite cellulose the increase in length of the crystalline region corresponds to one glucose ring, in MCC made from coniferous kraft cellulose it corresponds to nine rings, in MCC made from cellulose from flax fibres it corresponds to five rings (the increase between flax and cellulose from flax being six rings), and in cotton linter it corresponds to 24 rings. In spite of the large increase, the length of
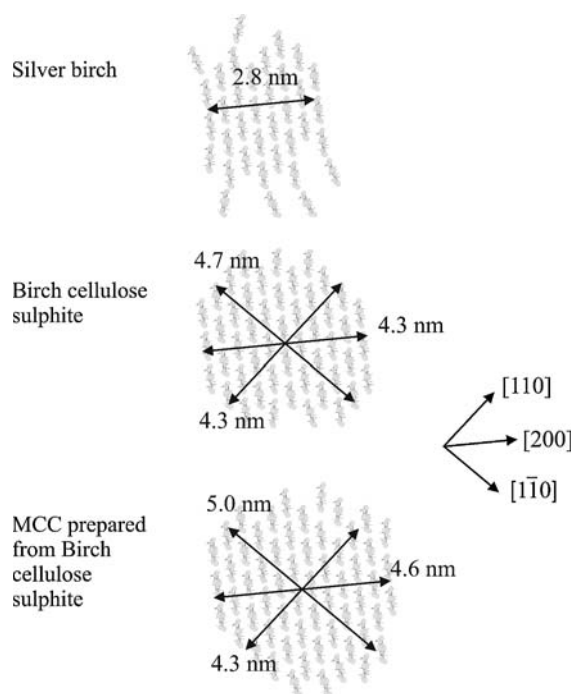

Fig. 9 A model for the cross section of the average crystalline region of the microfibril in birch wood (according to the results of Peura et al. 2009), birch sulphite pulp and MCC

crystalline regions in MCC from cotton linter, 30 nm, is still smaller than that of pristine wood, 35 nm. The changes in the length of the microfibril in spruce wood, kraft cooked coniferous cellulose and MCC made from it are presented in the Fig. 10.

The result, that the dimensions of the crystallites were larger in the MCC samples than in the starting materials, can be explained by the preparation of MCC. When making microcrystalline cellulose, residual hemicellulose and lignin are furthermore removed from the sample and this allows further surface chains to crystallize and the mean crystallite width to increase. The process conditions decrease DP and increase the chain mobility which allows crystallization also in the chain direction. DP is lowered during hydrolysis because the glycosidic linkages, which join the glucose monomers, are cleaved generating separate chain segments (Kato et al. 1999).

In the FTIR spectrum of cotton the band in the range 3000–3600 cm^{-1} was symmetric and the maximum was at 3430 cm^{-1}, and in the spectrum of cotton MCC the shape of the band became asymmetric and the maximum was shifted to 3380 cm^{-1}. Those facts were explained by removal of a part of the OH groups included to intramolecular bonds during hydrolysis. The FTIR spectrum of MCC from flax cellulose included similar peculiarities as the spectra of flax cellulose. The shape of the band in the range 3000–3600 cm^{-1} was the same as for flax cellulose and that band was also splitted to two bands with the same maxima. The FTIR spectra of MCC from birch cellulose, aspen and poplar pulp had similar shapes with each others. The bands in the range 3000–3600 cm^{-1} were symmetric and the maxima were at 3370, 3380 and 3390 cm^{-1}, respectively. Those maxima were slightly shifted to the lower frequencies compared to the corresponding pulp samples which may be connected to the increase of crystallite size and crystallinity (Table 2) during the hydrolysis.

Conclusions

In wood the average width of the crystalline core of the microfibrils agrees with the number of chains produced by a single rosette allowing also surface chains to be disordered. In cotton linter the size matches better with the number of chains produced

Fig. 10 A model for the changes in the length of the crystalline regions in the core of the microfibril in spruce wood (*left*), kraft cooked coniferous cellulose (*middle*) and MCC made from it (*right*). The total length of the last figure (MCC) corresponds to the measured DP of the sample
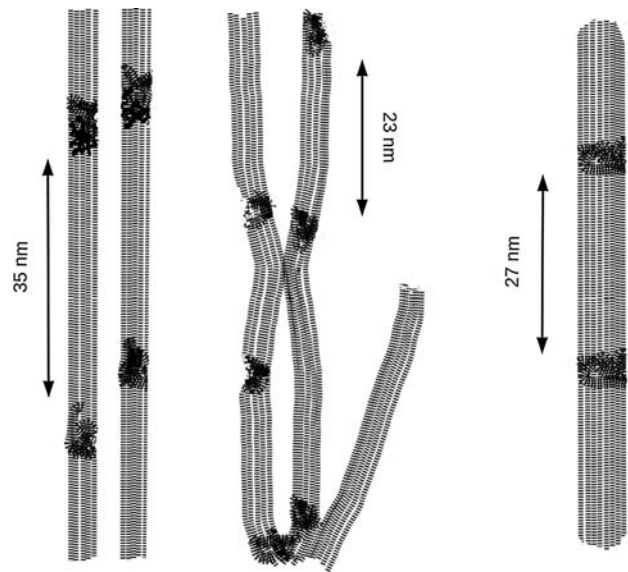
by two rosettes. This difference is explained by the smaller fractions of hemicellulose and lignin in cotton linter than in wood cell wall. However, the crystallites were considerably longer in wood with rigid fibre structures than in cotton linter.

The results shown in this paper indicate that from softwood or hardwood pulp, flax cellulose and cotton linter, MCC with very similar nanostructures were obtained. When making MCC from kraft or sulphite cooked wood, cotton linter or flax cellulose, the degree of polymerization decreased but the width and length of crystalline regions of cellulose microfibrils increased. This occurs via crystallization of the surface chains and aggregation of neighboring microfibrils. However, microfibrils did not become single crystals since the crystallinity in MCC samples was about 60%.

References

Andersson S (2007) A study of the nanostructure of the cell wall of the tracheids of conifer xylem by x-ray scattering. Ph.D. thesis, University of Helsinki. http://urn.fi/URN:ISBN:952-10-3235-9

Andersson S, Serimaa R, Torkkeli M, Paakkari T, Saranpää P, Pesonen E (2000) Microfibril angle of Norway spruce [*Picea abies* (L.) Karst.] compression wood: comparision of measuring techniques. J Wood Sci 46:343–349

Andersson S, Serimaa R, Paakkari T, Saranpää P, Pesonen E (2003) The crystallinity of wood and the size of cellulose crystallites in Norway spruce [*Picea abies* (L.) Karst]. J Wood Sci 49(6):531–537

Andersson S, Serimaa R, Väänänen T, Paakkari T, Jämsä S, Viitaniemi P (2005) X-ray scattering studies of thermally modified Scots pine (*Pinus sylvestris* L.). Holzforschung 59:422–427

Astley OM, Donald MA (2001) A small-angle x-ray scattering study of the effect of hydration on the microstructure of flax fibers. Biomacromolecules 2:672–680

Atalla RH, VanderHart DL (1984) Native cellulose—a composite of 2 distinct crystalline forms. Science 223(4633):283–285

Battista JA (1975) Microcrystal polymer science. McGraw-Hill Book Inc., USA, 208pp

Briki F, Busson B, Doucet J (1998) Organization of microfibrils in keratin fibers studied by X-ray scattering modelling using the paracrystal concept. Biochim Biophys Acta 1429:57–68

Buckton G, Yonemochi E, Moffat AC (1999) Water sorption and near IR spectroscopy to study the differences between microcrystalline cellulose and silicified microcrystalline cellulose before and after wet granulation. Int J Pharm 181(1):41

Busson B, Doucet J (1999) Distribution and interference functions for two-dimensional hexagonal paracrystals. Acta Cryst A 56:68–72

de Souza Lima MM, Borsali R (2004) Rodlike cellulose microcrystals: structure, properties and applications. Macromol Rapid Commun 25:771–787

Doblin MS, Kurek I, Jacob-Wilk D, Delmer DP (2002) Cellulose biosynthesis in plants: from genes to rosettes. Plant Cell Physiol 43(12):1407–1420

Donaldson L (2007) Cellulose microfibril aggregates and their size variation with cell wall type. Wood Sci Technol 41:443–460

Elazzouzi-Hafraoui S, Nishiyama Y, Putaux JL, Heux L, Dubreuil F, Rochas C (2008) The shape and size distribution of crystalline nanoparticles prepared by acid hydrolysis of native cellulose. Biomacromolecules 9:57–65

El-Sakhawy M, Hassan ML (2007) Physical properties of microcrystalline cellulose prepared from agricultural residues. Carbohydr Polym 67:1–10

Emons AM, Höfte H, Mulder BM (2007) Microtubules and cellulose microfibrils: how intimate is their relationship? Trends Plant Sci 12(7):279–281

Feigin LA, Svergun DI (1987) Structure analysis by small angle X-ray and neutron scattering. Plenum Press, New York, pp 90–94

Fengel D (1993) Structural changes of cellulose and their effects on the OH/CH2 valency vibration range in FTIR spectra. In: Kennedy JF, Phillips GO, Williams PA, Piculell I (eds) Cellulose and cellulose derivatives: physicochemical aspects and industrial applications. Woodhead Publ. Ltd, Cambridge, pp 75–84

Fleming K, Gray DG, Matthews S (2001) Cellulose crystallites. Chem Eur J 7(9):1831–1835

Fronk W, Wilke W (1985) Small angle scattering of partially oriented polymers: model calculations with monoclinic macrolattice. Colloid Polym Sci 263:97–108

Gomez LD, Steele-King CG, McQueen-Mason SJ (2008) Sustainable liquid biofuels from biomass: the writing's on the walls. New Phytol 178:473–485

Ioelovich M (1992) Zur übermolekularen Struktur von nativen und isolierten Cellulosen. Acta Polym 43:110–113

Jakob HF, Fengel D, Tschegg SE, Fratzl P (1995) The elementary cellulose fibril in *Picea abies*: comparison of transmission electron microscopy, small-angle X-ray scattering and wide-angle X-ray scattering results. Macromolecules 28:8782–8787

Jakob HF, Tschegg SE, Fratzl P (1996) Hydration dependence of the wood-cell structure in *Picea abies*. A small-angle scattering study. Macromolecules 29:8435–8440

Kato KL, Cameron RE (1999) A review of the relationship between thermally-accelerated ageing of paper and hornification. Cellulose 6:23–40

Knaapila M, Svensson C, Barauskas J, Zackrisson M, Nielsen SS, Toft KN, Vestergaard B, Arleth L, Olsson U, Pedersen JS, Cerenius Y (2009) A new small-angle X-ray scattering set-up on the crystallography beamline I711 at MAX-lab. J Synchrotron Rad (submitted)

Kotelnikova NE, Panarin EF (2005) Cellulose modification by biologically active substances for biomedical applications. Cellul Chem Technol 39(5–6):437–450

Kotelnikova NE, Petropavlovsky GA, Shevelev VA, Vasil'eva GG, Volkova LA (1976) Interaction of microcrystalline cellulose with water. Cellul Chem Technol 4(10):391–399

Kotelnikova NE, Petropavlovsky GA, Hou Y (1991) Hydrolytic destruction and properties of bleached and unbleached cellulose samples from deciduous wood samples (aspen and poplar). In: Chemistry and delignification of cellulose. Zinatne, Riga, pp 79–88

Kotelnikova NE, Panarin EF, Serimaa R, Paakkari T, Sukhanova TE, Gribanov AV (2000) Study of flax fibres structure by WAXS, IR- and ^{13}C NMR spectroscopy and SEM. In: Kennedy JF, Lonnberg B (eds) Cellulosic pulps, fibres and materials. Woodhead Publ. Ltd, Cambridge, pp 169–180

Krässig HA (1993) Cellulose: structure, accessibility, and reactivity. Gordon and Breach Science Publishers, USA, 376pp

Lotfy M, El-osta M, Kellogg RM, Foschi RO, Butters RG (1974) A mechanistic approach to crystallite length as related to cell-wall structure. Wood Fiber 6:36–45

Lundgren C (2004) Cell wall thickness and tangential and radial diameter of fertilized and irrigated Norway spruce. Silva Fenn 38(1):95–106

Matsuoka H, Tanaka H, Hashimoto T, Ise N (1987) Elastic scattering from cubic lattice systems with paracrystalline distortion. Phys Rev B 36:1754–1765

Mu XQ (1998) X-ray diffraction by a one-dimensional paracrystal of limited size. Acta Cryst A 54:606–616

Nishiyama Y, Langan P, Chanzy H (2002) Crystal structure and hydrogen-bonding system in cellulose Iβ from synchrotron x-ray and neutron fiber diffraction. J Am Chem Soc 124(31):9074–9082

Nishiyama Y, Kim UJ, Kim DY, Katsumata KS, May RP, Langan P (2003a) Periodic disorder along ramie cellulose microfibrils. Biomacromolecules 4:1013–1017

Nishiyama Y, Sugiyama Y, Chanzy H, Langan P (2003b) Crystal structure and hydrogen bonding system in cellulose Iα from synchrotron x-ray and neutron fiber diffraction. J Am Chem Soc 125(47):14300–14306

Pedersen JS (1997) Analysis of small-angle scattering data from colloids and polymer solutions: modeling and least-squares fitting. Adv Colloid Interface Sci 70:171–210

Petropavlovsky GA, Kotelnikova NE (1985) Phenomenological model of fine cellulose structure on the basis of the study of heterogeneous and homogeneous destruction. Acta Polym 36(2):118–123

Petropavlovsky GA, Kotelnikova NE, Pogodina TE (1980) Study of the structure and chromatographic properties of microcrystalline cellulose samples from birch wood. Wood Chem 6:3–12

Peura M, Grotkopp I, Lemke H, Vikkula A, Laine J, Müller M, Serimaa R (2006) Negative Poisson ratio of crystalline cellulose in kraft cooked Norway spruce. Biomacromolecules 7:1521–1528

Peura M, Müller M, Vainio U, Sarén MP, Saranpää P, Serimaa R (2007) X-ray microdiffraction reveals the orientation of cellulose microfibrils and the size of cellulose crystallites in single Norway spruce tracheids. Trees Struct Funct. doi:10.1007/s00468-007-0168-5

Peura M, Andersson S, Salmi A, Karppinen T, Torkkeli M, Hæggström E, Serimaa R (2009) Changes in nanostructure of wood cell wall during deformation. Adv Mater Sci Wood Mat Sci Forum. doi:10.4028/3-908453-08-9.126

Revol JF, Bradford H, Giasson J, Marchessault RH, Gray DG (1992) Helicoidal self-ordering of cellulose microfibrils in aqueous suspension. Int J Biol Macromol 14:170–172

Revol JF, Godbout L, Dong XM, Gray DG, Chanzy H, Maret G (1994) Chiral nematic suspensions of cellulose crystallites

phase separation and magnetic field orientation. Liq Cryst 16(1):127–134

Roman M, Gray DG (2005) Parabolic focal conics in self-assembled solid films of cellulose nanocrystals. Langmuir 21:5555–5561

Salmén L (2004) Micromechanical understanding of the cell-wall structure. C R Biol 327:873–880

Samir MASA, Alloin F, Dufresne A (2005) Review of recent research into cellulosic whiskers, their properties and their application in nanocomposite field. Biomacromolecules 6:612–626

Sjöström E (1993) Wood chemistry, fundamentals and applications, 2nd edn. Academic Press, San Diego

Sugiyama J, Vuong R, Chanzy H (1991) Electron diffraction study on the two crystalline phases occurring in native cellulose from an algal cell wall. Macromolecules 24(14):4168–4175

Tanaka F, Koshijima T, Okamura K (1981) Characterization of cellulose in compression and opposite woods of a *Pinus densiflora* tree grown under the influence of strong wind. Wood Sci Technol 15(4):265–273

Terech P, Chazeau L, Cavaille JY (1999) A small-angle scattering study of cellulose whiskers in aqueous suspensions. Macromolecules 32:1872–1875

Wilke W (1983) General lattice factor of the ideal paracrystal. Acta Cryst A 39:864–867

Wilke W, Bratrich M (1991) Investigation of the superstructure of polymers during deformation by synchrotron radiation. J Appl Cryst 24:645–650

Zografi G, Kontny MJ, Yang AYS, Brenner GS (1984) Surface area and water vapor sorption of macrocrystalline cellulose. Int J Pharm 18:99–116